Helicon Plasma Thruster Experiment Controlling Cross-Field Diffusion within a Magnetic Nozzle

IEPC-2013-163

Presented at the 33rd International Electric Propulsion Conference,
The George Washington University • Washington, D.C. • USA
October 6 – 10, 2013

K. Takahashi[1]
Department of Electrical Engineering, Tohoku University, Sendai, 980-8579, Japan

C. Charles[2] and R.W. Boswell[3]
Space Plasma, Power and Propulsion Laboratory, Research School of Physics and Engineering, The Australian National University, Canberra ACT 0200, Australia

and

A. Ando[4]
Department of Electrical Engineering, Tohoku University, Sendai, 980-8579, Japan

Abstract: Laboratory experiment of a helicon plasma thruster is established to control only the plasma cross-field diffusion in a rapidly-divergent magnetic nozzle, while maintaining a constant plasma injection into the magnetic nozzle. The thrust is equal in magnitude and opposite in direction to the force imparted to the thruster structure. The force components imparted to axial and radial source boundaries and to the magnetic nozzle are independently measured with changing the cross-field diffusion and the resultant plasma flow in the magnetic nozzle. The results show a constant force to the axial boundary, a negligible force to the radial boundary, and an increasing force to the magnetic nozzle, with an increasing the field strength of the magnetic nozzle. Further, the thrust measurements measured for various thruster configurations are performed.

Nomenclature

T_s	=	force exerted to the axial source boundary (back plate)
T_w	=	force exerted to the radial source boundary (glass source tube)
T_B	=	force exerted to the magnetic nozzle
r	=	radial position
r_s	=	source tube radius
z	=	axial position
z_0	=	axial position giving the maximum electron pressure
p_e	=	electron pressure
z_{end}	=	axial position of the back plate
m	=	ion mass

[1] Associate Professor, Department of Electrical Engineering, Tohoku University, kazunori@ecei.tohoku.ac.jp
[2] Professor, Space Plasma, Power and Propulsion, Research School of Physics and Engineering, The Australian National University, christine.charles@anu.edu.au
[3]Professor, Space Plasma, Power and Propulsion, Research School of Physics and Engineering, The Australian National University, rod.boswell@anu.edu.au
[4] Professor, Department of Electrical Engineering, Tohoku University, akira@ecei.tohoku.ac.jp

u = ion fluid velocity
B = magnetic field
r, z, θ = cylindrical coordinate index

I. Introduction

OVER the past few decades, various electric propulsion devices such as the ion gridded thruster, hall effect thruster, Magneto-Plasma-Dynamic thruster have been developed and successfully tested in space [1]. The new concept for electrodeless plasma thruster called 'helicon plasma thruster' is recently investigated theoretically [2,3] and experimentally [4-7]. The helicon plasma discharge can be operated over wide ranges of external parameters (rf power, rf frequency in the range of MHz, operating gas pressures, magnetic field) and can yield high plasma densities in the 10^{12}-10^{13} cm^{-3} range. The system simply consists of an insulator source tube surrounded by a radiofrequency antenna and a magnetic nozzle, which can be produced by solenoids and/or permanent magnets. The recent experiment using a cylindrical source verified the enhancement of the thrust by the magnetic nozzle, due to a Lorenz force originating from an azimuthal plasma current in the applied radial magnetic field [6]. The comparison between the experiments and calculations suggest that the main contribution to the plasma current is the electron diamagnetic current. In addition, the presence of additional thrust in the conical source structure is also suggested [7]. The physics relating to the thruster performance, which is arising from the physical boundaries and the magnetic nozzle, have not been fully understood yet. Some studies have suggested the analytical or numerical modeling of the thruster performance [3,8]; these results have not been compared with experiments yet.

Here measurements of the thrust imparted from the helicon plasma thrusters are performed. The thrust is equal in magnitude and opposite in direction to the force exerted onto the thruster structure including the magnetic nozzle. The laboratory experiment is designed to measure independently the force components exerted to the axial source boundary, to the radial source boundary, and to the magnetic nozzle. Further, the thrust for various configurations including a permanent magnet helicon plasma thruster are measured.

II. Independent measurement of the thrust components

In this section, the analytical model of the thrust imparted from the magnetic nozzle helicon plasma thruster is briefly shown, detail of which can be found in Ref.[9] and the independent measurements of the thrust components arising from the axial and radial source boundaries and from the magnetic nozzle are described. Some of results have already been reported by authors.

A. Analytical thrust model

The thrust can be derived from momentum equations of ions and electrons, which can be found in the previous study [9], assuming negligible electron inertia, negligible radial ion inertia, cold ions, and an axisymmetric plasma flow. Electron pressure forces onto the axial boundary (back plate) and magnetic nozzle have been incorporated in a previously described one-dimensional model [2], where the force onto the magnetic nozzle has been derived based on area expansion of the plasma cross section. The strong effect of the Lorentz force due to the radial magnetic field and the electron diamagnetic drift current has been experimentally observed and quantified [6], and the equivalence between a physical area expansion effect and the Lorentz force has been mathematically demonstrated [10]. The total force T_{total} onto the bounded plasma system including the magnetic nozzle is given by $T_{total} = T_s + T_w + T_B$, where

$$T_s = 2\pi \int_0^{r_s} r p_e(r, z_0) dr, \cdots (1)$$

$$T_w = -2\pi \int_{z_{end}}^{0} r_s m n_w u_r(r_s, z)\, u_z(r_s, z) dz, \cdots (2)$$

$$T_B = -2\pi \int_0^z \int_0^{rp} r \frac{B_r}{B_z} \frac{\partial p_e}{\partial r} dr dz. \cdots (3)$$

r_s, r_p, p_e, z_0, n_w, u are the source radius, plasma radius, electron pressure (=$n_p k_B T_e$, where n_p, k_B, and T_e are the plasma density, Boltzmann constant, and electron temperature), maximum pressure position, ion density at the radial boundary, and ion velocity, respectively. The T_s component is the maximum electron pressure in the source tube and converted into the ion dynamic momentum acting to the axial source boundary by the sheath acceleration. This is also equivalent to the axial momentum of the plasma at the plasma production position. This validity has already been demonstrated by using a simple inductively-coupled plasma thruster [11]. The T_w component is the radial

surface integration of the axial momentum lost by the ions escaping to the radial source boundary. In the previous theoretical model [12], this term is assumed to be negligible as the ions near the radial source boundary is generally axially slow ions. The T_B component is the Lorentz force arising from the radial magnetic field B_r and the azimuthal plasma current, which mainly originates from the electron diamagnetic drift current ($1/B_z * \partial p_e/\partial r$). As these three force components T_s, T_w, T_B are exerted to the axial source boundary, the radial source boundary, and the magnetic field lines, these can be experimentally identified by measuring the forces to these mechanical components (Source back plate, source tube, solenoid coil providing the magnetic field).

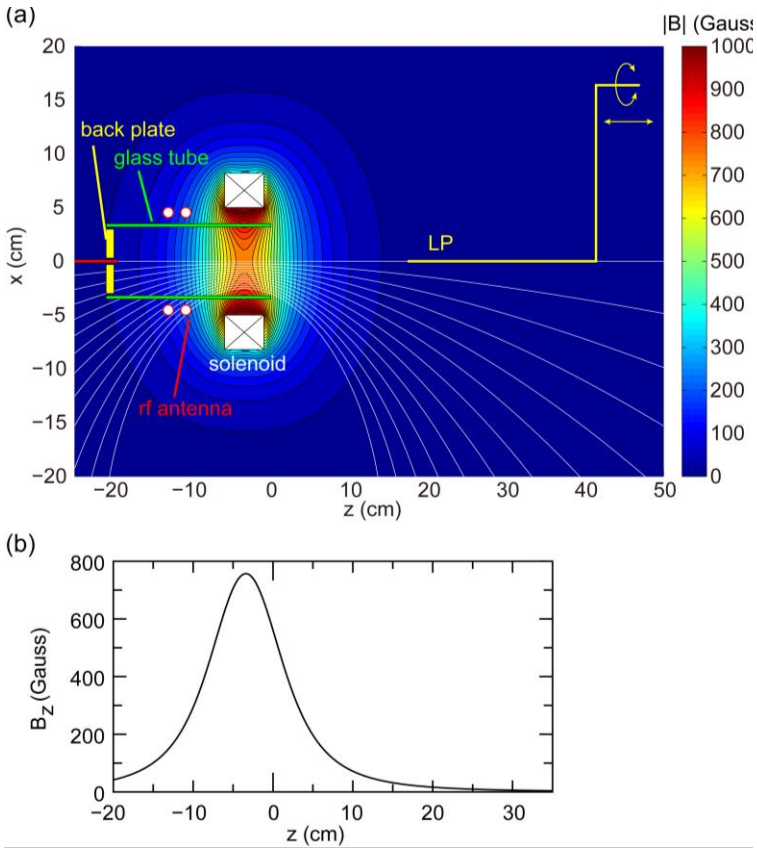

Figure 1. (a)Schematic diagram of the helicon plasma thruster being used presently. The magnetic field strength and field lines for the solenoid current of 15 A are shown by contour color and white lines. (b) Axial profile of the magnetic field strength on axis for the 15A solenoid current.

B. Experimental setup

Figure 1(a) shows the schematic diagram of the presently used helicon plasma thruster. The thruster is attached to a pendulum thrust balance immersed in a 60 cm diameter and 140 cm long vacuum chamber evacuated to a base pressure of 1 x 10^{-6} Torr by a turbomolecular/rotary pumping system. The thruster source cavity is a 6.4 cm diameter and 20 cm long pyrex glass tube. z = 0 is defined as the open exit of the source tube and the upstream end of the source cavity is terminated by an insulator back plate (z = -20 cm) with a 6 mm diameter center hole. Argon propellant is introduced via the center hole of the back plate using a 1 mm inner diameter and 2 mm outer diameter ceramic tube. The flow rate is controlled by a mass flow controller and the argon flow rate is maintained at 25 sccm; then the chamber pressure measured by a baratron gauge connected to the side port of the chamber is 0.8 mTorr. A 10 cm inner diameter, 16.4 cm outer diameter and 5 cm wide solenoid with 560 turns is located at z = -3.4 cm to provide a magnetic nozzle, where the solenoid current can be increased up to 15 A. The calculated magnetic field strength $|B|$ and the field lines are shown by contour color and white lines in Fig. 1(a), respectively. Figure 2(b) shows the axial profile of the magnetic field strength on axis for the same solenoid current as in Fig. 1(a). The magnetic field peaks at about 760 Gauss at the axial center of the solenoid (z = -3.4 cm) and rapidly decreases towards the upstream and downstream side of the plasma cavity. A double-turn rf loop antenna is situated at z = -11.5 cm and powered by a 13.56 MHz rf power supply and the argon plasma is produced. The rf power for the plasma production is maintained at 1 kW in the present experiment. To prevent the parasitic discharges around the rf antenna outside of the source cavity, the antenna is shielded by a thick ceramic ring and grounded metallic parts as described previously [13].

The electron temperature and plasma density in the source cavity balances the particle loss and energy loss with the ionization and input energy. As the magnetic field strength at the rf antenna position is less than 200 Gauss even for the maximum solenoid current, which gives the ion Larmor radius of above 2 cm comparable to the source radius, the plasma loss rate near the production position is expected to be unchanged by the magnetic field strength. Hence it is guessed that the plasma production is maintained at constant when changing the magnetic field strength in the range less than 15 A. On the other hand, the radial physical boundary (vacuum tank) is larger than the ion Larmor radius. Then the radial plasma diffusion across the magnetic field is expected to be affected by the field strength; only the cross field diffusion in the magnetic nozzle can be controlled by the solenoid current. As seen in

Eqs. (1)-(3), the absolute value of the solenoid current does not affect the thrust value directly, as the factor B_r/B_z is unchanged by the solenoid current. It is expected that only the plasma flow dynamics contribute to the absolute value of the thrust.

As described in Sec. II.A, the thrust components T_s, T_w, T_B are equal in magnitude and opposite in direction to the forces exerted to the axial source boundary (back plate), to the radial source boundary (glass source tube), and to the magnetic nozzle (solenoid), respectively. These independent measurements are performed by attaching either the back plate or the glass source tube or the solenoid to the pendulum thrust balance. The total thrust is also experimentally identified by the force measurement by attaching all the three components to the thrust balance. The displacement measured during turning on the plasma and the calibration coefficient relating the displacement to the force gives the absolute value of the force components.

C. Experimental results

To verify the control of only the cross field diffusion with a constant plasma production, the density measurements are performed at z = -12 cm (plasma production position) and z = 30 cm (in the magnetic nozzle), respectively, where the axial profiles of the plasma density have shown the maximum at z = -12 cm (not shown here and can be found in Ref. [14]). The density at z = -12 cm is found to be unchanged by the solenoid current, i.e., the magnetic field strength as expected in Sec. II. A, while the density at z = -30 cm increases with the increase in the magnetic field strength. This result shows that the cross field diffusion within the magnetic nozzle is inhibited by the stronger magnetic field strength and the higher plasma density in the magnetic nozzle is obtained, while maintaining the constant plasma production in the source cavity. Hence the presently designed source demonstrates the independent control of the cross-field diffusion with the constant plasma injection into the magnetic nozzle.

Figure 2 (b) shows the directly measured thrust components T_s (filled squares), T_w (open squares), T_B (open circles) and T_{total} (filled circles) as a function of the solenoid current. The T_s components is found to be fairly constant when changing the magnetic field strength; this is because that T_s relates to only the maximum electron pressure as seen in Eq. (1) and the constant plasma density inside the source cavity is obtained as seen in Fig. 2(a).

The directly measured T_w in Fig. 2(b) shows the value close to zero for the solenoid current larger than 1 A. This result validates the assumption that the radially lost ions do not deliver significant axial momentum to the radial source boundary for the magnetic nozzle plasma thruster. For the solenoid current less than 1 A, the negative force is

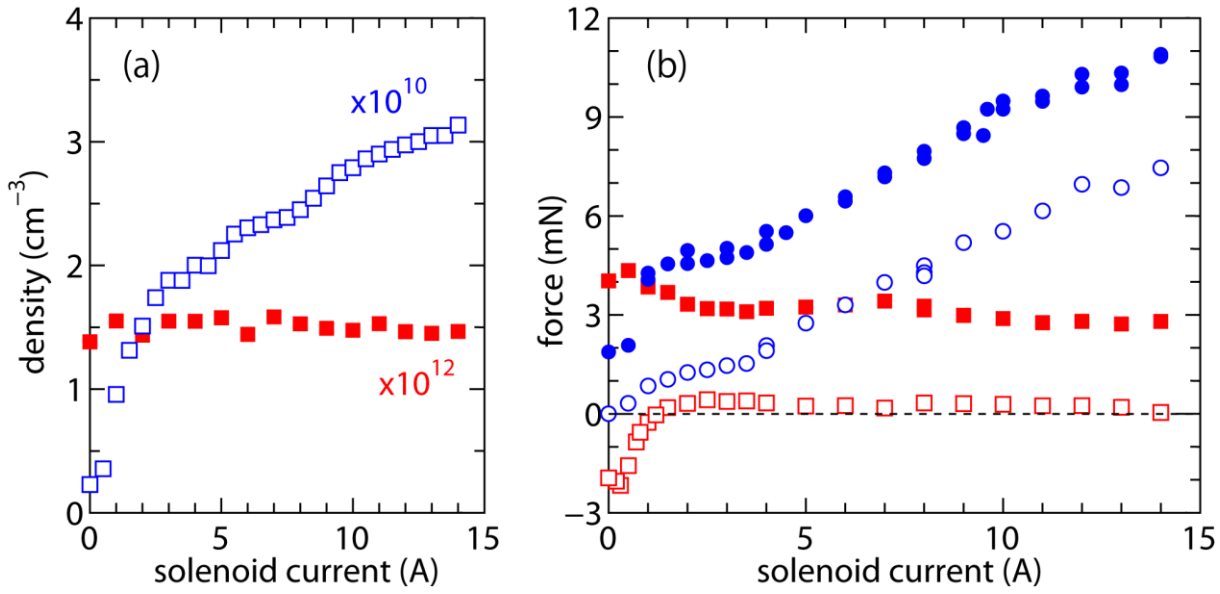

Figure 2. (a) Plasma density on axis measured at z = -12 cm (filled squares) and z = 30 cm (open squares) as a function of the solenoid current. (b) Thrust components T_s (filled squares), T_w (open squares), T_B (open circles) as a function of the solenoid current, together with the total thrust T_{total} (filled circles), which are directly measured by the pendulum thrust balance. Dashed line shows the zero thrust level for visual guide. These data are from Ref. [14].

detected as seen in Fig. 2(b). Although the detailed and quantified analysis has not been done yet, the measurement of the T_w component will give some important information relating to the particle dynamics and momentum transport near the source boundary.

The T_B component clearly increases with the increase in the solenoid current, which provide the inhibition of the cross field diffusion and the higher electron pressure within the magnetic nozzle as observed in Fig. 2(a). This is consistent with Eq. (3), which describes that T_B is proportional to the absolute value of the electron pressure within the magnetic nozzle. As the total thrust is given by the sum of the three thrust components (T_s, T_w, T_B), the total thrust also increases with the increase in the magnetic field strength. Hence it is demonstrated that the inhibition of the cross field diffusion significantly affects the thruster performance due to the contribution of T_B term. Here it should be noted that the sum of the directly measured T_s, T_w, and T_B agrees with the directly measured T_{total}. This validates the measurements made in the present experiment.

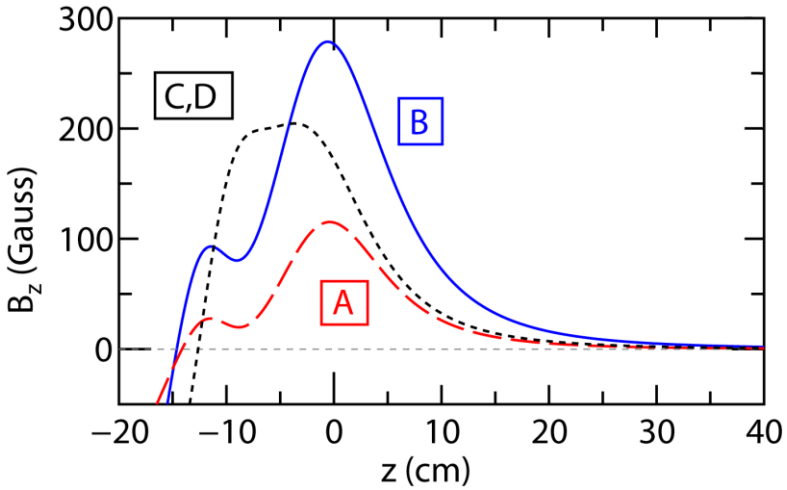

Figure 3. Axial profiles of the magnetic field strength on axis for the thruster configuration of "A-D" in Table 1.

III. Performance characterization

In this section, the solenoid to provide the magnetic nozzle is replaced by the permanent magnets (PMs) and the thruster performance is characterized by the direct measurement of T_{total} for several configuration of the thruster. The detailed configuration of the permanent magnets can be found in Ref. [15]. Briefly, double concentric arrays of the permanent magnets surrounds the source tube and can provide the axial magnetic field inside the source tube and the expanding magnetic field near the thruster exit. Typical thruster configurations are shown in Table 1, where the configuration in Sec. II (solenoid magnetic nozzle) is labeled "E" and the magnetic field for "A-D" configurations are provided by the PMs. The calculated axial profiles of the magnetic field for "A-D" configurations are plotted in Fig. 3. Here two type of the magnetic nozzle are tested; one has a uniform magnetic field within the source cavity and divergent magnetic field near the thruster exit (labeled as "*Uni-Div*" in Table 1), and another has a convergent magnetic field within the source cavity and divergent field near the thruster exit (labeled as "*Con-Div*" in table 1).

Figure 4 shows the directly measured thrust as a function of the rf power for the configurations "A" (open circles), "B" (open squares), "C" (crosses), "D" (filled triangles), "E" (filled circles), respectively. The data for "A-D" configurations are from Ref. [15]. It is found that the configuration "B" with the PMs has a similar thrust value to the solenoid type thruster "E" and the thrust of ~15

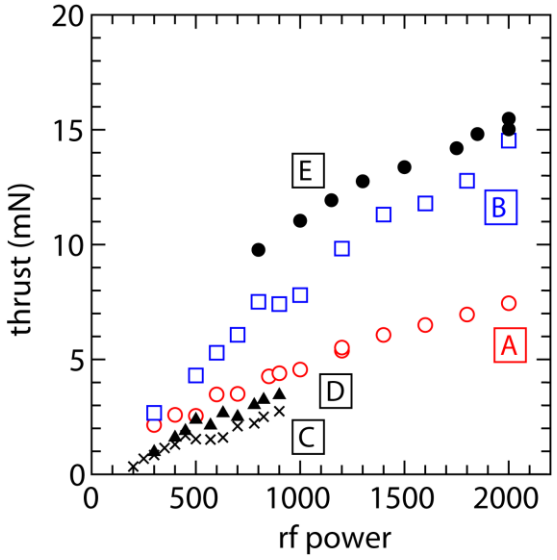

Figure 4. Directly measured thrust for the thruster configurations "A" (open circles), "B" (open squares), "C" (crosses), "D" (filled triangles), "E" (filled circles), respectively, as a function of the rf power. The data for "A-D" configurations are from Ref. [15]

Table 1. Thruster configurations being tested.

Thruster type	A	B	C	D	E
Cavity length (cm)	12	12	17.5	8	20
Cavity radius (cm)	6.5	6.5	6.5	6.5	6.5
Nozzle Configuration	*Con-Div*	*Con-Div*	*Uni-Div*	*Uni-Div*	*Con-Div*
Magnet type	PMs	PMs	PMs	PMs	Solenoid
Maximum field (Gauss)	~115	~275	~200	~200	~755
Gas flow rate (sccm)	24	24	20	31.3	25

 # Con-Div: Convergent-Divergent magnetic nozzle
 # Uni-Div: Uniform-Divergent magnetic nozzle

mN can be obtained for the rf power of 2 kW. However, it should be mentioned that the magnetic field strength for the configuration "B" (275 Gauss) is smaller than that for "E" (755 Gauss). The similar performance even for the smaller magnetic field is probably due to the shorter length of the source cavity, which gives the higher energy density of the rf power deposited to the plasma. As the use of the PMs requires no any electricity and no power supply for dc solenoid current, it will lead the higher performance of the thruster system.

IV. Conclusion

In conclusion, only the cross-field diffusion within the magnetic nozzle is successfully controlled with maintaining the constant plasma injection into the magnetic nozzle in the presently designed helicon plasma thruster; the thrust components arising from the axial and radial source boundaries and from the magnetic nozzle are independently measured. The results show that the inhibition of the cross field diffusion and the resultant higher electron pressure within the magnetic nozzle lead the significant improvement of the thruster performance. Further, the thrusts imparted from the various configurations of the thruster including the permanent magnet helicon plasma thruster are characterized experimentally. The presently obtained thrust is about 15 mN for 2 kW rf power.

Acknowledgments

This works is partially supported by a Grant-in-Aid for Scientific Research (B 25287150) from JSPS and Hattori Hokokai Foundation.

References

[1]Gobel D.M. and Katz I., *Fundamentals of Electric Propulsion: Ion and Hall thrusters*, John Wiley & Sons, New Jersey, 2008.

[2]Fruchtman A., "Electric Field in a Double Layer and the Imparted Momentum", *Physical Review Letters,* Vol. 96, February 2006, pp. 065002-1 – 4.

[3]Ahedo E. and Merino M., "Two-Dimensional Supersonic Plasma Acceleration in a Magnetic Nozzle", *Physics of Plasmas,* Vol. 17, July 2010, pp. 073501-1 – 15.

[4]Takahashi K., Lafleur T., Charles C., Alexander P., Boswell R.W., Perren M., Laine R., Pottinger S., Lappas V., Harle T., and Lamprou D., "Direct Thrust Measurement of a Permanent Magnet Helicon Double Layer Thruster", *Applied Physics Letters,* Vol. 98, April 2011, pp. 141503-1 – 3.

[5]Pottinger S., Lappas V., Charles C., and Boswell R., "Performance Characterization of a Helicon Double Layer Thruster Using Direct Thrust Measurements", *Journal of Physics D: Applied Physics,* Vol. 44, May 2011, pp. 235201-1 – 5.

[6]Takahashi K., Lafleur T., Charles C., Alexander P., and Boswell R., "Electron Diamagnetic Effect on Axial Force in an Expanding Plasma: Experiments and Theory", *Physical Review Letters,* Vol. 107, November 2011, pp. 235001-1 – 5.

[7]Charles C., Takahashi K., and Boswell R., "Axial Force Imparted by a Conical Radiofrequency Magneto-Plasma Thruster", *Applied Physics Letters,* Vol. 100, March 2012, pp. 113504-1 – 3.

[8]Ahedo E. and Navarro-Cavallé J., "Helicon Thruster Plasma Modeling: Two-Dimensional Fluid-Dynamics and Propulsive Performances", *Physics of Plasmas,* Vol. 20, April 2013, pp. 043512-1 – 13.

[9]Takahashi K., Lafleur T., Charles C., Alexander P., and Boswell R.W., "Axial Force Imparted by a Current-Free Magnetically Expanding Plasma", *Physics of Plasmas*, Vol. 19, August 2012, pp. 083509-1 – 8.

[10]Fruchtman A., Takahashi K., Charles C., and Boswell R.W., "A Magnetic Nozzle Calculation of the Force on a Plasma", *Physics of Plasmas*, Vol. 19, March 2012, pp. 033507-1 – 6.

[11]Lafleur T., Takahashi K., Charles C., and Boswell R.W., "Direct Thrust Measurements and Modelling of a Radio-Frequency Expanding Plasma Thruster", *Physics of Plasmas*, Vol. 18, August 2012, pp. 080701-1 – 4.

[12]Fruchtman A., "Neutral Depletion in a Collisionless Plasma", *IEEE Transactions on Plasma Science*, Vol. 36, April 2008, pp. 403 – 413.

[13]Takahashi K., "Radiofrequency antenna for Suppression of Parasitic Discharges in a Helicon Plasma Thruster Experiment", *Review of Scientific Instruments*, Vol. 83, August 2012, pp. 083508-1 – 4.

[14]Takahashi K., Charles C., and Boswell R.W., "Approaching the Theoretical Limit of Diamagnetic-Induced Momentum in a Rapidly Diverging Magnetic Nozzle", *Physical Review Letters*, Vol. 110, May 2013, pp. 195003-1 – 5.

[15]Takahashi K., Charles C., Boswell R.W., and Ando A., "Performance Improvement of a Permanent Magnet Helicon Plasma Thruster", *Journal of Physics D: Applied Physics*, Vol. 46, August 2013, pp. 352001-1 – 5.